Lecture 4: High oscillations

Table of contents

This lecture[1] deals with numerical approaches for second order Hamiltonian systems with highly oscillatory solutions. We focus on the situation where the product of time step size and highest frequency in the system is not small.

1 A Fermi–Pasta–Ulam type problem

The problem of Fermi, Pasta & Ulam[2] (see also the recent lecture notes[3]) is a simple model for simulations in statistical mechanics which revealed highly unexpected dynamical behaviour. We consider a modification consisting of a chain of m mass points, connected with alternating soft nonlinear and stiff linear springs, and fixed at the end points (see Galgani, Giorgilli, Martinoli & Vanzini[4] and Figure 1). The variables $q_1, \dots, q_{2m}$ ($q_0 = q_{2m+1} = 0$) stand for the displacements

[1] Large parts are taken from "Geometric Numerical Integration" by Hairer, Lubich & Wanner.

[2] E. Fermi, J. Pasta & S. Ulam, *Studies of non linear problems.* Los Alamos Report No. LA-1940 (1955), later published in E. Fermi: Collected Papers (Chicago 1965), and Lect. Appl. Math. 15, 143 (1974).

[3] G. Gallavotti (ed.), *The Fermi–Pasta–Ulam problem.* Lecture Notes in Physics, vol. 728, Springer, Berlin, 2008. A status report.

[4] L. Galgani, A. Giorgilli, A. Martinoli & S. Vanzini, *On the problem of energy equipartition for large systems of the Fermi–Pasta–Ulam type: analytical and numerical estimates*, Physica D 59 (1992), 334–348.

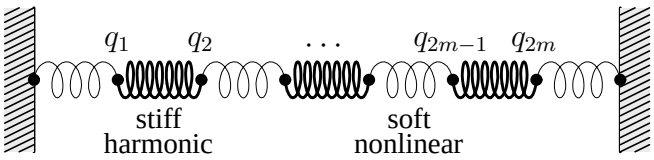

Figure 1: Chain with alternating soft nonlinear and stiff linear springs

of the mass points, and $p_i = \dot{q}_i$ for their velocities. The motion is described by a Hamiltonian system with total energy

$$H(p,q) = \frac{1}{2}\sum_{i=1}^{m}\big(p_{2i-1}^2 + p_{2i}^2\big) + \frac{\omega^2}{4}\sum_{i=1}^{m}(q_{2i} - q_{2i-1})^2 + \sum_{i=0}^{m}(q_{2i+1} - q_{2i})^4,$$

where ω is assumed to be large. With the symplectic change of coordinates

$$\begin{aligned} x_{0,i} &= \big(q_{2i} + q_{2i-1}\big)/\sqrt{2}, \qquad x_{1,i} = \big(q_{2i} - q_{2i-1}\big)/\sqrt{2}, \\ \dot{x}_{0,i} &= \big(p_{2i} + p_{2i-1}\big)/\sqrt{2}, \qquad \dot{x}_{1,i} = \big(p_{2i} - p_{2i-1}\big)/\sqrt{2}, \end{aligned} \tag{1}$$

where $x_{0,i}$ is a scaled displacement of the ith stiff spring, $x_{1,i}$ a scaled expansion (compression) of the ith stiff spring, we get a Hamiltonian system with

$$\begin{aligned} H(x,\dot{x}) \;=\; & \frac{1}{2}\sum_{i=1}^{m}\Big(\dot{x}_{0,i}^2 + \dot{x}_{1,i}^2\Big) + \frac{\omega^2}{2}\sum_{i=1}^{m} x_{1,i}^2 + \frac{1}{4}\Big((x_{0,1} - x_{1,1})^4 + \\ & + \sum_{i=1}^{m-1}\big(x_{0,i+1} - x_{1,i+1} - x_{0,i} - x_{1,i}\big)^4 + (x_{0,m} + x_{1,m})^4\Big). \end{aligned} \tag{2}$$

Besides the fact that the total energy is exactly conserved, the system has a further interesting feature. We consider the oscillatory energy

$$I = I_1 + \ldots + I_m, \qquad I_j = \frac{1}{2}\big(\dot{x}_{1,j}^2 + \omega^2 x_{1,j}^2\big), \tag{3}$$

where I_j denotes the harmonic energy of the jth stiff spring, and the kinetic energies corresponding to the slow and fast motions

$$T_0 = \frac{1}{2}\sum_{i=1}^{m}\dot{x}_{0,i}^2, \qquad T_1 = \frac{1}{2}\sum_{i=1}^{m}\dot{x}_{1,i}^2. \tag{4}$$

For an illustration we choose $m = 3$ (as in Figure 1), $\omega = 50$, $x_{0,1}(0) = 1$, $\dot{x}_{0,1}(0) = 1$, $x_{1,1}(0) = \omega^{-1}$, $\dot{x}_{1,1}(0) = 1$, and zero for the remaining initial values. Figure 2 shows the different time scales that are present in the evolution of the system.

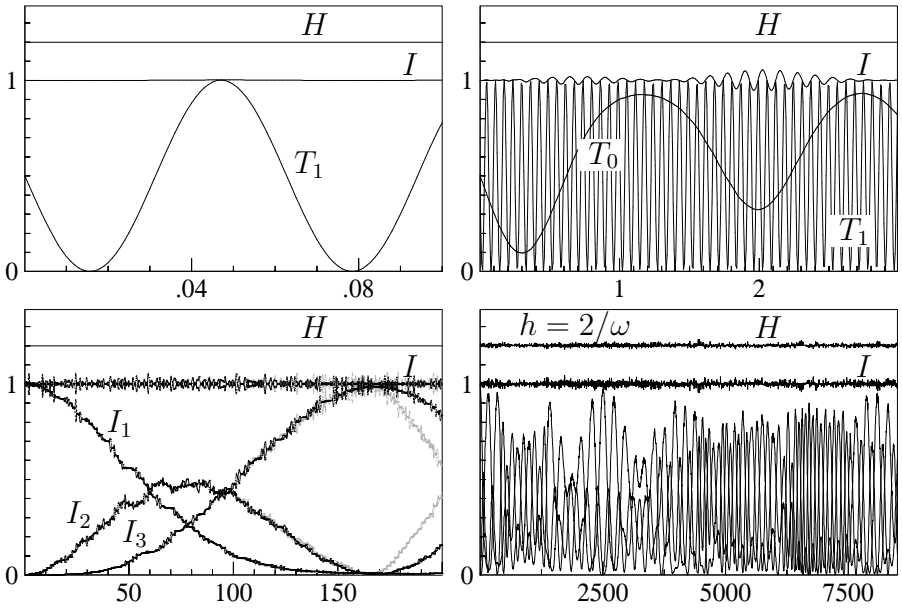

Figure 2: Different time scales in the FPU type problem ($\omega = 50$).

Time Scale ω^{-1}. The vibration of the stiff linear springs is nearly harmonic with almost-period π/ω. This is illustrated by the plot of T_1 in the first picture.

Time Scale ω^0. This is the time scale of the motion of the soft nonlinear springs, as is exemplified by the plot of T_0 in the second picture of Figure 2.

Time Scale ω. A slow energy exchange among the stiff springs takes place on the scale ω. In the third picture (see also the zoom to the right), the initially excited first stiff spring passes energy to the second one, and then also the third stiff spring begins to vibrate. The picture also illustrates that the problem is very sensitive to perturbations of the initial data: the grey curves of each of I_1, I_2, I_3 correspond to initial data where 10^{-5} has been added to $x_{0,1}(0)$, $\dot{x}_{0,1}(0)$ and $\dot{x}_{1,1}(0)$. The displayed solutions of the first three pictures have been computed very accurately by an adaptive integrator.

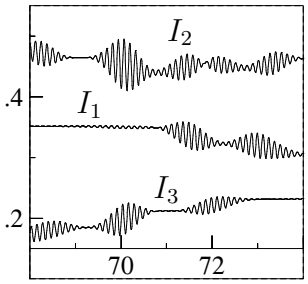

Time Scale ω^N, $N \geq 2$. The oscillatory energy I has only $\mathcal{O}(\omega^{-1})$ deviations from the initial value over very long time intervals. The fourth picture of Figure 2 shows the total energy H and the oscillatory energy I as computed by an exponential integrator (see Section 3) with step size $h = 2/\omega = 0.04$, which is nearly as large as the time interval of the first picture. No drift is seen for H or I.

2 Application of classical integrators

Which of the methods, discussed in Lecture 2, produce qualitatively correct approximations when the product of the step size h with the high frequency ω is relatively large?

Linear stability analysis. To get an idea of the maximum admissible step size, we neglect the nonlinear term in the differential equation, so that it splits into the two-dimensional problems $\dot{y}_{0,i} = 0$, $\dot{x}_{0,i} = y_{0,i}$ and

$$\dot{y}_{1,i} = -\omega^2 x_{1,i}, \quad \dot{x}_{1,i} = y_{1,i}. \tag{5}$$

Omitting the subscripts, the solution of (5) is

$$\begin{pmatrix} y(t) \\ \omega\, x(t) \end{pmatrix} = \begin{pmatrix} \cos\omega t & -\sin\omega t \\ \sin\omega t & \cos\omega t \end{pmatrix} \begin{pmatrix} y(0) \\ \omega\, x(0) \end{pmatrix}.$$

The numerical solution of a one-step method applied to (5) yields

$$\begin{pmatrix} y_{n+1} \\ \omega\, x_{n+1} \end{pmatrix} = M(h\omega) \begin{pmatrix} y_n \\ \omega\, x_n \end{pmatrix}, \tag{6}$$

and the eigenvalues λ_i of $M(h\omega)$ determine the long-time behaviour of the numerical solution. Stability (i.e., boundedness of the solution of (6)) requires the eigenvalues to be less than or equal to one in modulus. For the explicit Euler method we have $\lambda_{1,2} = 1 \pm \mathrm{i}h\omega$, so that the energy $I_n = (y_n^2 + \omega^2 x_n^2)/2$ increases as $(1 + h^2\omega^2)^{n/2}$. For the implicit Euler method we have $\lambda_{1,2} = (1 \pm \mathrm{i}h\omega)^{-1}$, and the energy decreases as $(1 + h^2\omega^2)^{-n/2}$. For the implicit midpoint rule and for all symplectic Runge–Kutta methods, the matrix $M(h\omega)$ is orthogonal and therefore I_n is exactly preserved for all h and n. Finally, for the symplectic Euler method and for the Störmer–Verlet scheme we have

$$M(h\omega) = \begin{pmatrix} 1 & -h\omega \\ h\omega & 1 - h^2\omega^2 \end{pmatrix}, \quad M(h\omega) = \begin{pmatrix} 1 - \frac{h^2\omega^2}{2} & -\frac{h\omega}{2}\Big(1 - \frac{h^2\omega^2}{4}\Big) \\ \frac{h\omega}{2} & 1 - \frac{h^2\omega^2}{2} \end{pmatrix}.$$

For both matrices, the characteristic polynomial is $\lambda^2 - (2 - h^2\omega^2)\lambda + 1$, so that the eigenvalues are of modulus one if and only if $|h\omega| \leq 2$.

Numerical experiments. We apply several methods to the FPU type problem, with $\omega = 50$ and initial data as in Figure 2. Figure 3 presents the numerical results for $H - 0.8$, I, I_1, I_2, I_3 (the last picture only for I and I_2) obtained with the implicit midpoint rule, the classical Runge–Kutta method of order 4, and the Störmer–Verlet scheme. For the small step size $h = 0.001$ all methods give satisfactory results, although the energy exchange is not reproduced accurately

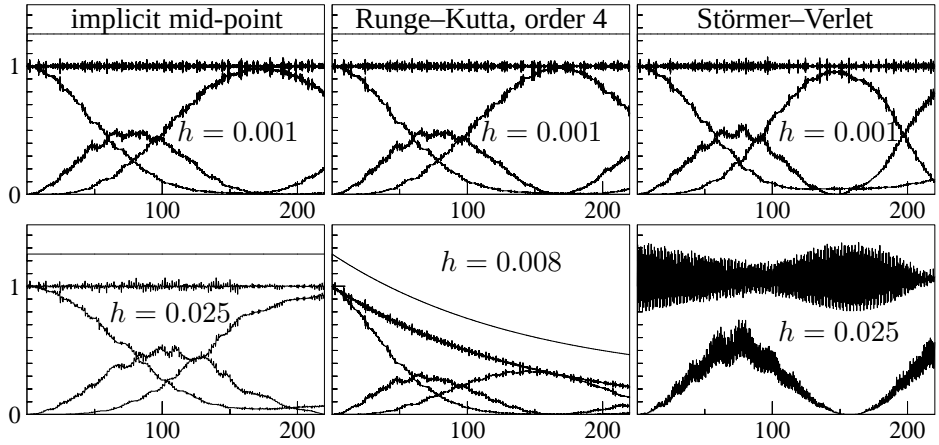

Figure 3: Numerical solution for the FPU problem (2) with data as in Figure 2.

over long times (compare with exact solution in Figure 2). The explicit Runge–Kutta method gives completely wrong solutions for larger step sizes (or for small step sizes and larger time intervals). The values of H and I are still bounded over very long time intervals for the Störmer–Verlet method, but the relative error is very large for step sizes close to the stability limit ($h = 0.025$ corresponds to $h\omega = 1.25$). These phenomena call for an explanation, and for numerical methods with an improved behaviour.

3 Exponential (trigonometric) integrators

The Störmer–Verlet scheme for $\ddot{x} = g(x)$ is obtained by replacing the second derivative with the difference $h^{-2}(x_{n+1} - 2x_n + x_{n-1})$. For a differential equation

$$\ddot{x} + \Omega^2 x = g(x), \quad g(x) = -\nabla U(x), \quad \Omega = \begin{pmatrix} 0 & 0 \\ 0 & \omega I \end{pmatrix} \tag{7}$$

we replace the linear part by

$$h^{-2}\big(x_{n+1} - 2\,\cos(h\Omega)\,x_n + x_{n-1}\big),$$

which reproduces the exact solution for $\ddot{x} + \Omega^2 x = 0$. The derivative of the exact solution for this linear problem satisfies (with $\mathrm{sinc}(\xi) = \sin\xi/\xi$)

$$2h\,\mathrm{sinc}(h\Omega)\,\dot{x}(t) \;=\; x(t+h) - x(t-h),$$

which leads to an approximation of the derivative.

Two-step formulation. We consider numerical integrators of the form

$$\begin{aligned} x_{n+1} - 2\cos(h\Omega)\, x_n + x_{n-1} &= h^2 \Psi g(\Phi x_n) \\ 2h\,\mathrm{sinc}(h\Omega)\,\dot{x}_n &= x_{n+1} - x_{n-1}. \end{aligned} \tag{8}$$

Here $\Psi = \psi(h\Omega)$ and $\Phi = \phi(h\Omega)$, where the *filter functions* ψ and ϕ are bounded, even, real-valued functions with $\psi(0) = \phi(0) = 1$. In our numerical experiments we will consider the following choices of ψ and ϕ

(A)	$\psi(\xi) = \mathrm{sinc}^2(\frac{1}{2}\xi)$	$\phi(\xi) = 1$	Gautschi[1]
(B)	$\psi(\xi) = \mathrm{sinc}(\xi)$	$\phi(\xi) = 1$	Deuflhard[2]
(C)	$\psi(\xi) = \mathrm{sinc}(\xi)\,\phi(\xi)$	$\phi(\xi) = \mathrm{sinc}(\xi)$	García-Archilla & al.[3]
(D)	$\psi(\xi) = \mathrm{sinc}^2(\frac{1}{2}\xi)$	$\phi(\xi)$ of [4]	Hochbruck & Lubich[4]
(E)	$\psi(\xi) = \mathrm{sinc}^2(\xi)$	$\phi(\xi) = 1$	Hairer & Lubich[5]

One-step formulation. Eliminating x_{n-1} from the two relations in (8), we obtain the following equations

$$x_{n+1} = \cos h\Omega\, x_n + \Omega^{-1} \sin h\Omega\, \dot{x}_n + \tfrac{1}{2} h^2 \Psi\, g_n \tag{9}$$

$$\dot{x}_{n+1} = -\Omega \sin h\Omega\, x_n + \cos h\Omega\, \dot{x}_n + \tfrac{1}{2} h \big(\Psi_0\, g_n + \Psi_1\, g_{n+1}\big) \tag{10}$$

where $g_n = g(\Phi x_n)$ and $\Psi_0 = \psi_0(h\Omega)$, $\Psi_1 = \psi_1(h\Omega)$ with even functions ψ_0, ψ_1 defined by

$$\psi(\xi) = \mathrm{sinc}(\xi)\,\psi_1(\xi)\,, \qquad \psi_0(\xi) = \cos(\xi)\,\psi_1(\xi). \tag{11}$$

Method (9)-(10) is of order 2 (for $h \to 0$), and it is symmetric whenever (11) is satisfied. The method is symplectic if in addition (see Exercise 2)

$$\psi(\xi) = \mathrm{sinc}(\xi)\,\phi(\xi). \tag{12}$$

---

[1] W. Gautschi, *Numerical integration of ordinary differential equations based on trigonometric polynomials*, Numer. Math. 3 (1961) 381–397.

[2] P. Deuflhard, *A study of extrapolation methods based on multistep schemes without parasitic solutions*, Z. angew. Math. Phys. 30 (1979) 177–189.

[3] B. García-Archilla, J.M. Sanz-Serna & R.D. Skeel, *Long-time-step methods for oscillatory differential equations*, SIAM J. Sci. Comput. 20 (1999) 930–963.

[4] M. Hochbruck & Ch. Lubich, *A Gautschi-type method for oscillatory second-order differential equations*, Numer. Math. 83 (1999a) 403–426.

[5] E. Hairer & Ch. Lubich, *Long-time energy conservation of numerical methods for oscillatory differential equations*, SIAM J. Numer. Anal. 38 (2000) 414-441.

Energy exchange between stiff components. Figure 4 shows the energy exchange of the six methods (A)-(F) applied to the FPU problem with the same data as in Figure 2. The figures show again the oscillatory energies I_1, I_2, I_3 of the stiff springs, their sum $I = I_1+I_2+I_3$ and the total energy $H-0.8$ as functions of time on the interval $0 \leq t \leq 200$. Only the methods (B), (D) and (F) give a good approximation of the energy exchange between the stiff springs. By the use of mod-

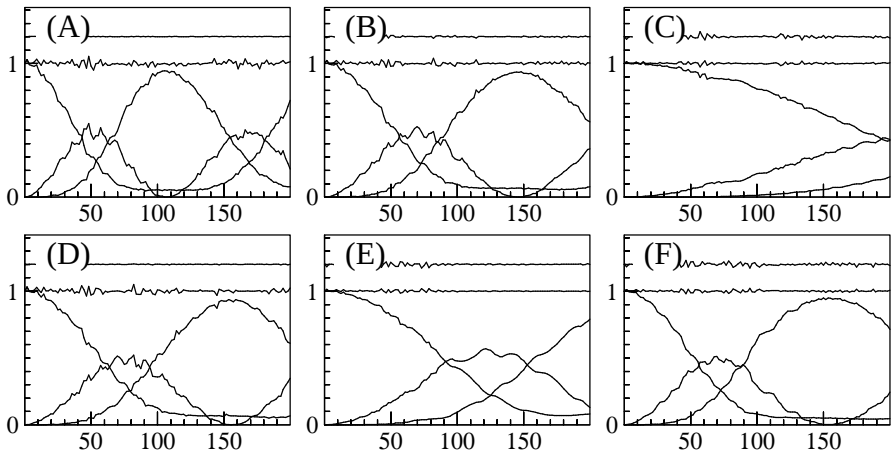

Figure 4: Energy exchange between stiff springs for methods (A)-(F) ($h = 0.035$, $\omega = 50$). Method (F) is not considered in these notes.

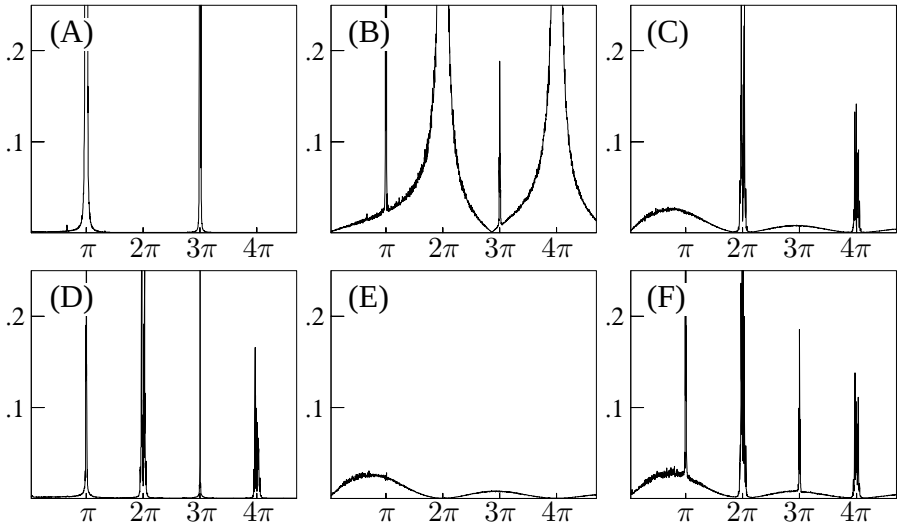

Figure 5: Maximum error of the total energy on the interval $[0, 1000]$ for methods (A) - (F) as a function of $h\omega$ (step size $h = 0.02$).

ulated Fourier expansions (see below) it can be shown that a necessary condition for a correct approximation of the energy exchange is $\psi(h\omega)\phi(h\omega) = \mathrm{sinc}(h\omega)$, which is satisfied for method (B). The good behaviour of method (D) comes from the fact that here $\psi(h\omega)\phi(h\omega) \approx 0.95\,\mathrm{sinc}(h\omega)$ for $h\omega = 1.5$.

Near-conservation of total and oscillatory energies. Figure 5 shows the maximum error of the total energy H as a function of the scaled frequency $h\omega$ (step size $h = 0.02$). We consider the long time interval $[0, 1000]$. The pictures for the different methods show that in general the total energy is well conserved. Exceptions are near integral multiples of π. Certain methods show a bad energy conservation close to odd multiples of π, other methods close to even multiples of π. Only method (E) shows a uniformly good behaviour for all frequencies. In

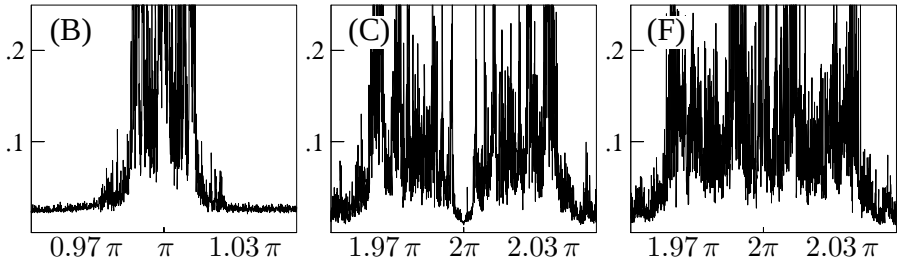

Figure 6: Zoom (close to π or 2π) of the maximum error of the total energy on the interval $[0, 1000]$ for three methods as a function of $h\omega$ (step size $h = 0.02$).

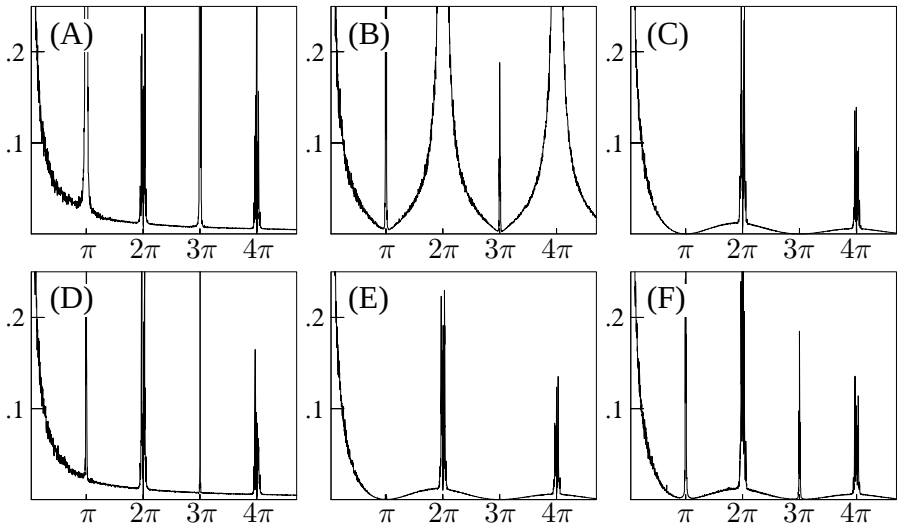

Figure 7: Maximum deviation of the oscillatory energy on the interval $[0, 1000]$ for methods (A) - (F) as a function of $h\omega$ (step size $h = 0.02$).

Figure 6 we show in more detail what happens close to such integral multiples of π. If there is a difficulty close to π, it is typically in an entire neighbourhood. Close to 2π, the picture is different. Method (C) has good energy conservation for values of $h\omega$ that are very close to 2π, but there are small intervals to the left and to the right, where the error in the total energy is large. Unlike the other methods shown, method (B) has poor energy conservation in rather large intervals around even multiples of π. Methods (A) and (D) conserve the total energy particularly well, for $h\omega$ away from integral multiples of π.

Figure 7 shows similar pictures where the total energy H is replaced by the oscillatory energy I. For the exact solution we have $I(t) = Const + \mathcal{O}(\omega^{-1})$. It is therefore not surprising that this quantity is not well conserved for small values of ω. None of the considered methods conserves both quantities H and I uniformly for all values of $h\omega$.

4 Modulated Fourier expansion

Let us consider second order ordinary differential equations

$$\ddot{x} + \Omega^2 x = g(x), \quad g(x) = -\nabla U(x), \quad \Omega = \begin{pmatrix} 0 & 0 \\ 0 & \omega I \end{pmatrix}. \tag{13}$$

To motivate a suitable ansatz for the solution, we notice that the general solution of $\ddot{x} + \omega^2 x = 0$ is $x(t) = c_1 \mathrm{e}^{\mathrm{i}\omega t} + c_{-1}\mathrm{e}^{-\mathrm{i}\omega t}$, that of $\ddot{x} + \omega^2 x = x$ is $x(t) = \mathrm{e}^{\mathrm{i}\omega t} z^1(t) + \mathrm{e}^{-\mathrm{i}\omega t} z^{-1}(t)$ with $z^{\pm 1}(t) = c_{\pm 1}\mathrm{e}^{\pm \mathrm{i}\alpha t}$ and $\alpha = \sqrt{\omega^2 + 1} - \omega = \mathcal{O}(\omega^{-1})$. If $g(x)$ contains quadratic terms, also products of $\mathrm{e}^{\pm \mathrm{i}\omega t} z^{\pm 1}(t)$ will be involved.

Modulated Fourier expansion of the exact solution. We aim in writing the solution of (13) as

$$x(t) = \sum_{k \in \mathbb{Z}} \mathrm{e}^{\mathrm{i}k\omega t} z^k(t), \qquad z^k(t) = \begin{pmatrix} z_0^k(t) \\ z_1^k(t) \end{pmatrix}, \tag{14}$$

where the coefficient functions $z^k(t)$ are partitioned according to the partitioning of Ω in (13). This expansion is called *modulated Fourier expansion*[5] of the solution. It is essential that the coefficient functions $z^k(t)$ do not contain high oscillations. More precisely, we search for functions such that the derivatives of $z^k(t)$ up to a certain order are bounded uniformly when $\omega \to \infty$.

[5] E. Hairer & Ch. Lubich, *Long-time energy conservation of numerical methods for oscillatory differential equations*, SIAM J. Numer. Anal. 38 (2000) 414-441.

Inserting the expansion (14) into the differential equation (13), and comparing the coefficients of $\mathrm{e}^{\mathrm{i}k\omega t}$ yields (for $\omega_0 = 0$, $\omega_1 = \omega$)

$$\ddot{z}_j^k + 2\mathrm{i}k\omega\dot{z}_j^k + \big(\omega_j^2 - (k\omega)^2\big)z_j^k = \sum_{s(\alpha)=k} \frac{1}{m!}\, g_j^{(m)}(z^0)(z^{\alpha_1}, \dots, z^{\alpha_m}), \qquad (15)$$

where the sum ranges over all $m \geq 0$ and all multi-indices $\alpha = (\alpha_1, \dots, \alpha_m)$ with $\alpha_j \neq 0$, having a given sum $s(\alpha) = \sum_{j=1}^m \alpha_j$. Among the solutions of these second order differential equations we have to select those, whose derivatives are uniformly bounded in ω. To achieve this, we determine the dominant term in the left-hand side of (15) for $\omega \to \infty$, put the other terms to the right-hand side, and eliminate higher derivatives by iteration until a sufficiently high order. In this way we get

- a second order differential equation for $z_0^0(t)$,
- first order differential equations for $z_1^{\pm 1}(t)$,
- algebraic equations for all other $z_j^k(t)$.

This construction can best be understood by first studying the smooth solution of problems like $\ddot{z} + \omega^2 z = g(t)$ or $\ddot{z} + 2\mathrm{i}\omega\dot{z} = g(t)$.

Initial values for the differential equations are obtained from (14) and its derivative taken at $t = 0$:

$$x(0) = \sum_{k\in\mathbb{Z}} z^k(0), \qquad \dot{x}(0) = \sum_{k\in\mathbb{Z}} \Big(\mathrm{i}k\omega z^k(0) + \dot{z}^k(0)\Big).$$

Using the above algebraic relations for $z_j^k(t)$ and the differential equations for $z_1^{\pm 1}(t)$, these equations constitute a nonlinear system that defines uniquely $z_0^0(0)$, $\dot{z}_0^0(0)$, $z_1^{\pm 1}(0)$ as functions of $x(0)$ and $\dot{x}(0)$. This construction yields a unique (formal) expansion of the form (14) for the initial value problem (13). Because of the non-convergence of the series, they have to be truncated by neglecting terms of size $\mathcal{O}(\omega^{-N-1})$.

The above construction shows that under the *bounded-energy condition* for the initial values,

$$\frac{1}{2}\big(\|\dot{x}(0)\|^2 + \|\Omega x(0)\|^2\big) \leq E, \qquad (16)$$

the coefficient functions of (14) satisfy on a finite time interval $0 \leq t \leq T$,

$$\begin{array}{lll} z_0^0 = \mathcal{O}(1), & z_0^{\pm 1} = \mathcal{O}(\omega^{-3}), & z_0^k = \mathcal{O}(\omega^{-k-2}) \\ z_1^0 = \mathcal{O}(\omega^{-2}), & z_1^{\pm 1} = \mathcal{O}(\omega^{-1}), & z_1^k = \mathcal{O}(\omega^{-k-2}). \end{array} \qquad (17)$$

Modulated Fourier expansion of the numerical solution. To get insight into the numerical solution of

$$x_{n+1} - 2\cos h\Omega\, x_n + x_{n-1} = h^2 \Psi g(\Phi x_n) \tag{18}$$

we aim in writing the numerical solution as $x_n = x_h(nh)$ with

$$x_h(t) \;=\; \sum_{k\in\mathbb{Z}} \mathrm{e}^{\mathrm{i}k\omega t} z_h^k(t). \tag{19}$$

As we proceeded for the analytic solution, we insert the ansatz (19) into the numerical method (18) and compare the coefficients of $\mathrm{e}^{\mathrm{i}k\omega t}$. Using the relation

$$\begin{aligned} x_h(t+h) + x_h(t-h) \;=\; \sum_{k\in\mathbb{Z}} \mathrm{e}^{\mathrm{i}k\omega t}\Big(& 2\,\cos(k\omega h)\big(z_h^k(t) + \tfrac{h^2}{2!}\ddot z_h^k(t) + \ldots\big) \\ & + 2\mathrm{i}\,\sin(k\omega h)\big(h\dot z_h^k(t) + \tfrac{h^3}{3!}\dddot z_h^k(t) + \ldots\big)\Big). \end{aligned}$$

and the abbreviations $c^k = \cos(\frac{h}{2}k\omega)$, $s_j^k = \mathrm{sinc}(\frac{h}{2}(\omega_j - k\omega))$ we obtain[6]

$$\begin{aligned} \ldots + \tfrac{2\mathrm{i}}{3}\, s_0^{2k} k\omega h^2 \dddot z_j^k + c^{2k}\ddot z_j^k + 2\mathrm{i} s_0^{2k} k\omega \dot z_j^k + s_j^k s_j^{-k}(\omega_j^2 - (k\omega)^2) z_j^k \\ = \sum_{s(\alpha)=k} \frac{1}{m!}\, \Psi_j g_j^{(m)}(\Phi z^0)(\Phi z^{\alpha_1}, \ldots, \Phi z^{\alpha_m}), \end{aligned}$$

which reduces to (15) in the limit $h \to 0$. Again we have to determine the dominant terms in the right-hand side – this time asymptotically for $h \to 0$ and $h\omega \geq c > 0$, so that $\omega^{-1} = \mathcal{O}(h)$. Under the numerical non-resonance condition

$$|\sin(\tfrac{1}{2}k\omega h)| \geq c\sqrt{h} \quad \text{for} \quad k = 1, \ldots, N \tag{20}$$

we get a system of differential and algebraic equations for z_j^k. As before, we get a second order differential equation for $z_0^0(t)$, first order differential equations for $z_1^{\pm 1}(t)$, and algebraic relations for the other $z_j^k(t)$. Also initial values are obtained in the same way as for the analytic solution. To avoid the difficulty with the non-convergence of the arising series, we truncate them by neglecting terms of size $\mathcal{O}(h^{N+1})$. Under suitable assumptions on the filter functions, the coefficients of the modulated Fourier expansion are bounded as follows:

$$\begin{aligned} & z_0^0 = \mathcal{O}(1), \qquad z_0^{\pm 1} = \mathcal{O}(\omega^{-2}), \qquad z_0^k = \mathcal{O}(\omega^{-k}) \\ & z_1^0 = \mathcal{O}(\omega^{-2}), \quad z_1^{\pm 1} = \mathcal{O}(\omega^{-1}), \qquad z_1^k = \mathcal{O}(\omega^{-k}). \end{aligned} \tag{21}$$

[6]Components of the functions $z^k(t)$ of (19) are written without the subscript h. Notice, nevertheless, that they are different from those of (14). We want to avoid a further subscript, and hope that there will not arise any confusion.

An expansion for the derivative $\dot{x}_n = x_h'(nh)$ can be immediately obtained by inserting (19) into the second equation of (8). Notice that $x_h'(t)$ is not the time derivative of $x_h(t)$.

5 Invariants of the modulated Fourier expansion

The equation (13) is a Hamiltonian system with the Hamiltonian

$$H(x,\dot{x}) \;=\; \frac{1}{2}\big(\dot{x}^T\dot{x} + x^T\Omega^2 x\big) + U(x), \tag{22}$$

and we have seen in the numerical experiments that the quantity

$$I(x,\dot{x}) \;=\; \frac{1}{2}\big(\|\dot{x}_1\|^2 + \omega^2\|x_1\|^2\big) \tag{23}$$

plays an important role.

Invariants for the exact solution. In the modulated Fourier expansion of the analytic solution $x(t)$, denote $y^k(t) = e^{\mathrm{i}k\omega t}z^k(t)$ for all k, and collect them in

$$\mathbf{y} = (\dots, y^{-2}, y^{-1}, y^0, y^1, y^2, \dots).$$

By (15) these functions satisfy

$$\ddot{y}^k + \Omega^2 y^k \;=\; -\sum_{s(\alpha)=k} \frac{1}{m!}\, U^{(m+1)}(y^0)\big(y^{\alpha_1},\dots,y^{\alpha_m}\big). \tag{24}$$

The important and somewhat surprising observation is that with the expression

$$\mathcal{U}(\mathbf{y}) \;=\; U(y^0) + \sum_{s(\alpha)=0} \frac{1}{m!}\, U^{(m)}(y^0)\big(y^{\alpha_1},\dots,y^{\alpha_m}\big) \tag{25}$$

the differential equation for $\mathbf{y}(t)$ obtains the Hamiltonian structure

$$\ddot{y}^k + \Omega^2 y^k \;=\; -\nabla_{y^{-k}}\,\mathcal{U}(\mathbf{y}). \tag{26}$$

This system does not only have the Hamiltonian as a first integrals, but it has the following two (formal) first integrals:

$$\begin{aligned} \mathcal{H}(\mathbf{y},\dot{\mathbf{y}}) &= \frac{1}{2}\sum_{k\in\mathbb{Z}}\Big((\dot{y}^{-k})^T\dot{y}^k + (y^{-k})^T\Omega^2 y^k\Big) + \mathcal{U}(\mathbf{y}) \\ \mathcal{I}(\mathbf{y},\dot{\mathbf{y}}) &= -\,\mathrm{i}\,\omega\sum_{k\in\mathbb{Z}} k\,(y^{-k})^T\dot{y}^k. \end{aligned} \tag{27}$$

Theorem 1 *For a fixed N, and with a suitable truncation of the series in (25) and (27), we have*

$$\mathcal{H}(\mathbf{y}(t),\dot{\mathbf{y}}(t)) \;=\; \mathcal{H}(\mathbf{y}(0),\dot{\mathbf{y}}(0)) + \mathcal{O}(\omega^{-N}) \tag{28}$$

$$\mathcal{H}(\mathbf{y}(t),\dot{\mathbf{y}}(t)) \;=\; H(x(t),\dot{x}(t)) + \mathcal{O}(\omega^{-1}), \tag{29}$$

where the constants symbolized by $\mathcal{O}$ are independent of ω and t with $0 \le t \le T$, but depend on E of (16), N and T.

Similar estimates are obtained for the second invariant

$$\mathcal{I}(\mathbf{y}(t),\dot{\mathbf{y}}(t)) \;=\; \mathcal{I}(\mathbf{y}(0),\dot{\mathbf{y}}(0)) + \mathcal{O}(\omega^{-N}) \tag{30}$$

$$\mathcal{I}(\mathbf{y}(t),\dot{\mathbf{y}}(t)) \;=\; I(x(t),\dot{x}(t)) + \mathcal{O}(\omega^{-1}). \tag{31}$$

Proof. Taking the scalar product of (26) with $\dot{y}^{-k}$ and summing over all k shows that both sides become total derivatives. This leads to the explicit formula for $\mathcal{H}(\mathbf{y},\dot{\mathbf{y}})$. The proof of (30) is somewhat more tricky. We note that with the vector $\mathbf{y}(\lambda)$, whose components are $\mathrm{e}^{\mathrm{i}k\lambda}y^k$, the expression $\mathcal{U}(\mathbf{y}(\lambda))$ is independent of λ. Its derivative with respect to λ thus yields

$$0 \;=\; \frac{d}{d\lambda}\mathcal{U}(\mathbf{y}(\lambda))\Big|_{\lambda=0} \;=\; \sum_{k\in\mathbb{Z}} \mathrm{i}\,k\,(y^k)^T\,\nabla_k\,\mathcal{U}(\mathbf{y}), \tag{32}$$

for all $\mathbf{y}$. Using this relation, a multiplication of (26) with $k\,y^{-k}$ leads to the explicit formula for $\mathcal{I}(\mathbf{y},\dot{\mathbf{y}})$ which proves (30) after suitable truncation.

By the bounds (17), we have for $0 \le t \le T$

$$\mathcal{H}(\mathbf{y},\dot{\mathbf{y}}) = \tfrac{1}{2}\|\dot{y}_0^0\|^2 + \|\dot{y}_1^1\|^2 + \omega^2\|y_1^1\|^2 + U(y^0) + \mathcal{O}(\omega^{-1}). \tag{33}$$

On the other hand, we have from (23) and (14)

$$H(x,\dot{x}) = \tfrac{1}{2}\|\dot{y}_0^0\|^2 + \tfrac{1}{2}\|\dot{y}_1^1 + \dot{y}_1^{-1}\|^2 + \tfrac{1}{2}\omega^2\|y_1^1 + y_1^{-1}\|^2 + U(y^0) + \mathcal{O}(\omega^{-1}). \tag{34}$$

Using $y_1^1 = e^{i\omega t}z_1^1$ and $\dot{y}_1^1 = e^{i\omega t}(\dot{z}_1^1 + i\omega z_1^1)$ together with $y_1^{-1} = \overline{y_1^1}$, it follows from $\dot{z}_1^1 = \mathcal{O}(\omega^{-1})$ that $\dot{y}_1^1 + \dot{y}_1^{-1} = i\omega(y_1^1 - y_1^{-1}) + \mathcal{O}(\omega^{-1})$ and $\|\dot{y}_1^1\| = \omega\|y_1^1\| + \mathcal{O}(\omega^{-1})$. Inserted into (33) and (34), this yields (29).

Property (31) is obtained in the same way as for the Hamiltonian. □

Invariants for the numerical solution. We introduce the differential operator

$$\begin{aligned}\mathcal{L}(hD) \;&:=\; e^{hD} - 2\cos h\Omega + e^{-hD} \;=\; 2\big(\cos(ihD) - \cos h\Omega\big)\\ &=\; 4\,\sin^2\big(\tfrac{1}{2}h\Omega\big) + h^2D^2 + \frac{1}{12}\,h^4D^4\ldots\end{aligned} \tag{35}$$

so that the function $x_h(t)$ of (19) formally satisfies the difference scheme

$$\mathcal{L}(hD)x_h(t) \;=\; h^2\Psi g\big(\Phi x_h(t)\big). \tag{36}$$

We insert the modulated Fourier expansion $x_h(t) \;=\; \sum_k \mathrm{e}^{\mathrm{i}k\omega t}z_h^k(t) \;=\; \sum_k y_h^k(t)$

with $y_h^k(t) = \mathrm{e}^{\mathrm{i}k\omega t} z_h^k(t)$, expand the right-hand side into a Taylor series around $\Phi y_h^0(t)$, and compare the coefficients containing the factor $e^{\mathrm{i}k\omega t}$. This yields, for $g(x) = -\nabla U(x)$, the following formal equations for the functions $y_h^k(t)$,

$$\mathcal{L}(hD) y_h^k = -h^2 \Psi \sum_{s(\alpha)=k} \frac{1}{m!}\, U^{(m+1)}(\Phi y_h^0)\big(\Phi y_h^{\alpha_1}, \dots, \Phi y_h^{\alpha_m}\big), \tag{37}$$

which are the numerical analogue of (24). With the extended potential

$$\mathcal{U}_h(\mathbf{y}_h) \;=\; U(\Phi y_h^0) + \sum_{s(\alpha)=0} \frac{1}{m!}\, U^{(m)}(\Phi y_h^0)\big(\Phi y_h^{\alpha_1}, \dots, \Phi y_h^{\alpha_m}\big), \tag{38}$$

this system can be (formally) written as

$$\Psi^{-1}\Phi\, h^{-2} \mathcal{L}(hD)\, y_h^k \;=\; -\,\nabla_{-k}\, \mathcal{U}_h(\mathbf{y}_h). \tag{39}$$

The essential difference to the situation in (26) is the appearance of higher even derivatives in the left-hand expression.

To find a first invariant of the differential equation (39), we take its scalar product with $\dot y_h^{-k} = \overline{y_h^k}$, so that the right-hand side becomes the total derivative $\frac{d}{dt}\mathcal{U}(\mathbf{y}_h)$. Also the left-hand sides can be written as a total derivative, which is a consequence of relations of the type

$$\mathrm{Re}\, \dot{\overline{z}}^T z^{(2l)} \;=\; \mathrm{Re}\, \frac{d}{dt}\Big(\dot{\overline{z}}^T z^{(2l-1)} - \ldots \mp (\overline{z}^{(l-1)})^T z^{(l+1)} \pm \frac{1}{2}\, (\overline{z}^{(l)})^T z^{(l)} \Big).$$

To find a second invariant, we take the scalar product with $k\, y_h^{-k}$, and use an identity similar to that of (32), so that the right-hand side vanishes. To write the left-hand side as a total derivative we use

$$\mathrm{Im}\, \overline{z}^T z^{(2l+2)} \;=\; \mathrm{Im}\, \frac{d}{dt}\Big(\overline{z}^T z^{(2l+1)} - \dot{\overline{z}}^T z^{(2l)} + \ldots \pm (\overline{z}^{(l)})^T z^{(l+1)} \Big).$$

A careful elaboration of these ideas (see Section XIII.6 of our monograph on "Geometric Numerical Integration") we obtain the following result.

Theorem 2 *Under suitable assumptions on the filter functions and on the step size, which will be stated below in more detail, there exist functions $\mathcal{H}_h(\mathbf{y})$ and $\mathcal{I}_h(\mathbf{y})$ such that the following holds for $0 \le t = nh \le T$:*

$$\begin{aligned} \mathcal{H}_h\big(\mathbf{y}(t)\big) &= \mathcal{H}_h\big(\mathbf{y}(0)\big)\big) + \mathcal{O}(th^N)\,, \quad & \mathcal{I}_h\big(\mathbf{y}(t)\big) &= \mathcal{I}_h\big(\mathbf{y}(0)\big) + \mathcal{O}(th^N) \\ \mathcal{H}_h\big(\mathbf{y}(t)\big) &= H(x_n, \dot x_n) + \mathcal{O}(h), & \mathcal{I}_h\big(\mathbf{y}(t)\big) &= I(x_n, \dot x_n) + \mathcal{O}(h). \end{aligned}$$

The constants symbolized by $\mathcal{O}$ depend on the energy E, on the truncation index N and on T, but not on ω.

6 Long-time energy conservation

The statements of the preceding section are valid on intervals $[0, T]$, where T is a fixed value independent of ω. We show here how the results on energy conservation can be extended to much longer time intervals.

Conservation of the oscillatory energy for the analytic solution. Whereas the conservation of the total energy $H(x, \dot{x})$ along the analytic solution is obvious, the near-conservation of the oscillatory energy is a non-trivial, but typical feature of highly oscillatory problems.

Theorem 3 *If the solution $x(t)$ of (13) stays in a compact set for $0 \le t \le \omega^N$, then*

$$I(x(t), \dot{x}(t)) \;=\; I(x(0), \dot{x}(0)) + \mathcal{O}(\omega^{-1}) + \mathcal{O}(t\omega^{-N}) \; .$$

The constants symbolized by $\mathcal{O}$ are independent of ω and t with $0 \le t \le \omega^N$, but depend on the initial energy E and on the truncation index N.

Proof. With a fixed $T > 0$, let $\mathbf{y}_j$ denote the vector of the modulated Fourier expansion terms that correspond to starting values $(x(jT), \dot{x}(jT))$ on the exact solution. For $t = (n + \theta)T$ with $0 \le \theta < 1$, we have by Theorem 1,

$$\begin{aligned} I(x(t), \dot{x}(t)) &- I(x(0), \dot{x}(0)) \\ &= \; \mathcal{I}(\mathbf{y}_n(\theta T), \dot{\mathbf{y}}_n(\theta T)) + \mathcal{O}(\omega^{-1}) - \mathcal{I}(\mathbf{y}_0(0), \dot{\mathbf{y}}_0(0)) + \mathcal{O}(\omega^{-1}) \\ &= \; \mathcal{I}(\mathbf{y}_n(\theta T), \dot{\mathbf{y}}_n(\theta T)) - \mathcal{I}(\mathbf{y}_n(0), \dot{\mathbf{y}}_n(0)) + \\ &\quad \sum_{j=0}^{n-1} \Big(\mathcal{I}(\mathbf{y}_{j+1}(0), \dot{\mathbf{y}}_{j+1}(0)) - \mathcal{I}(\mathbf{y}_j(0), \dot{\mathbf{y}}_j(0)) \Big) + \mathcal{O}(\omega^{-1}) \; . \end{aligned}$$

We note

$$\mathcal{I}(\mathbf{y}_{j+1}(0), \dot{\mathbf{y}}_{j+1}(0)) - \mathcal{I}(\mathbf{y}_j(0), \dot{\mathbf{y}}_j(0)) \;=\; \mathcal{O}(\omega^{-N}) \; ,$$

because, by the quasi-uniqueness of the coefficient functions, we have for the truncated modulated Fourier expansion that $\mathbf{y}_{j+1}(0) \;=\; \mathbf{y}_j(T) + \mathcal{O}(\omega^{-N})$ and $\dot{\mathbf{y}}_{j+1}(0) = \dot{\mathbf{y}}_j(T) + \mathcal{O}(\omega^{-N})$. This yields the result. □

Energy conservation for the numerical solution. We are now able to prove one of the main results of this lecture – the near-conservation of the total energy H and the oscillatory energy I over long time intervals. In the previous section we emphasized the ideas without giving details on the assumptions for rigorous error estimates. We state them here without proof.

- the energy bound: $\frac{1}{2}\big(\|\dot{x}(0)\|^2 + \|\Omega x(0)\|^2\big) \le E$;

- the condition on the numerical solution: the values Φx_n stay in a compact subset of a domain on which the potential U is smooth;
- the conditions on the filter functions: ψ and ϕ are even, real-analytic, and have no real zeros other than integral multiples of π; furthermore, they satisfy $\psi(0) = \phi(0) = 1$ and

$$\begin{aligned} &|\psi(h\omega)| \;\le\; C_1 \operatorname{sinc}^2(\tfrac{1}{2}h\omega)\,, \qquad |\phi(h\omega)| \;\le\; C_2\,|\operatorname{sinc}(\tfrac{1}{2}h\omega)|\,, \\ &|\psi(h\omega)\phi(h\omega)| \;\le\; C_3\,|\operatorname{sinc}(h\omega)|\,; \end{aligned} \tag{40}$$

- the condition $h\omega \ge c_0 > 0$;
- the non-resonance condition (20): for some $N \ge 2$,

$$|\sin(\tfrac{1}{2}kh\omega)| \;\ge\; c\sqrt{h} \qquad \text{for} \quad k = 1, \ldots, N.$$

Theorem 4 *Under the above conditions, the numerical solution of (13) obtained by the method (9)–(10) with (11) satisfies, for* $0 \le nh \le h^{-N+1}$*,*

$$\begin{aligned} H(x_n, \dot{x}_n) \;&=\; H(x_0, \dot{x}_0) + \mathcal{O}(h) \\ I(x_n, \dot{x}_n) \;&=\; I(x_0, \dot{x}_0) + \mathcal{O}(h). \end{aligned}$$

The constants symbolized by $\mathcal{O}$ are independent of n, h, ω satisfying the above conditions, but depend on N and the constants in the conditions.

Proof. These long-time error bounds can be obtained as in the proof of Theorem 3. One only has to use the estimates of Theorem 2 instead of those of Theorem 1. □

7 Behavior of the Störmer–Verlet discretization

In applications, the Störmer–Verlet method is often used with step sizes h for which the product with the highest frequency ω is not small, so that backward error analysis does not provide any insight into the long-time energy preservation. For example, in spatially discretized wave equations, $h\omega$ is known as the CFL number, which is typically kept near 1. Values of $h\omega$ around 0.5 are often used in molecular dynamics simulations.

Consider now applying the Störmer–Verlet method to the nonlinear model problem (13),

$$\begin{aligned} x_{n+1} - 2x_n + x_{n-1} \;&=\; -\,h^2\Omega^2 x_n - h^2 \nabla U(x_n) \\ 2h\,\dot{x}_n \;&=\; x_{n+1} - x_{n-1} \end{aligned} \tag{41}$$

with $h\omega < 2$ for linear stability. The method is made accessible to the analysis

of the preceding sections by rewriting it as an exponential integrator

$$\begin{aligned} x_{n+1} - 2\cos(h\widetilde{\Omega})\, x_n + x_{n-1} &= -h^2 \nabla U(x_n) \\ 2h\,\mathrm{sinc}(h\widetilde{\Omega})\, x'_n &= x_{n+1} - x_{n-1} \end{aligned} \qquad \widetilde{\Omega} = \begin{pmatrix} 0 & 0 \\ 0 & \widetilde{\omega} I \end{pmatrix}. \tag{42}$$

with $\psi(\xi) = \phi(\xi) = 1$, and with *modified frequency* $\widetilde{\omega}$, defined by

$$1 - \frac{(h\omega)^2}{2} = \cos(h\widetilde{\omega}) \qquad \text{or, equivalently,} \qquad \sin\Big(\frac{h\widetilde{\omega}}{2}\Big) = \frac{h\omega}{2}.$$

The velocity approximation x'_n is related to $\dot{x}_n$ by

$$\dot{x}_n = \mathrm{sinc}(h\widetilde{\Omega})\, x'_n \qquad \text{or} \qquad \begin{aligned} \dot{x}_{n,0} &= x'_{n,0} \\ \dot{x}_{n,1} &= \mathrm{sinc}(h\widetilde{\omega})\, x'_{n,1}. \end{aligned} \tag{43}$$

Theorem 5 *Let the Störmer–Verlet method be applied to (13) with initial values satisfying (16), and with a step size h for which $0 < c_0 \le h\omega \le c_1 < 2$ and $|\sin(\frac{1}{2}kh\widetilde{\omega})| \ge c\sqrt{h}$ for $k = 1, \dots, N$ for some $N \ge 2$ and $c > 0$.*

Suppose further that the numerical solution values x_n stay in a region on which all derivatives of U are bounded. Then, we have for $0 \le nh \le h^{-N+1}$

$$\begin{aligned} H(x_n, \dot{x}_n) + \frac{\gamma}{2}\,\|\dot{x}_{n,1}\|^2 &= \mathit{Const} + \mathcal{O}(h) \\ I(x_n, \dot{x}_n) \;\; + \frac{\gamma}{2}\,\|\dot{x}_{n,1}\|^2 &= \mathit{Const} + \mathcal{O}(h) \end{aligned}$$

along the numerical solution, where

$$\gamma = \frac{(h\omega/2)^2}{1 - (h\omega/2)^2}$$

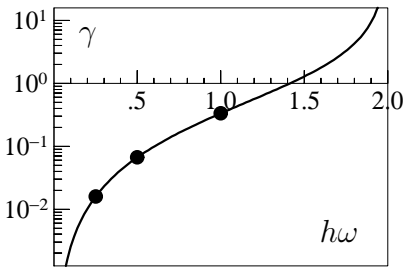

The constants symbolized by $\mathcal{O}$ are independent of n, h, ω with the above conditions.

Proof. The condition $0 < c_0 \le h\omega \le c_1 < 2$ implies $|\sin(\frac{1}{2}kh\widetilde{\omega})| \ge c_2 > 0$ for $k = 1, 2$, and hence conditions (40) are trivially satisfied with $h\widetilde{\omega}$ instead of $h\omega$. We are thus in the position to apply Theorem 4 to (42), which yields

$$\begin{aligned} \widetilde{H}(x_n, x'_n) &= \widetilde{H}(x_0, x'_0) + \mathcal{O}(h) \\ \widetilde{I}(x_n, x'_n) &= \widetilde{I}(x_0, x'_0) + \mathcal{O}(h) \end{aligned} \qquad \text{for } 0 \le nh \le h^{-N+1}\,, \tag{44}$$

where $\widetilde{H}$ and $\widetilde{I}$ are defined in the same way as H and I, but with $\widetilde{\omega}$ in place of ω.

With the relations (43) we get

$$\begin{aligned} \widetilde{I}(x_n, x'_n) &= \frac{1}{2}\Big(\|x'_{n,1}\|^2 + \widetilde{\omega}^2 \|x_{n,1}\|^2\Big) \\ &= \left(\frac{\widetilde{\omega}}{\omega}\right)^2 \left(I(x_n, \dot{x}_n) - \frac{1}{2}\|\dot{x}_{n,1}\|^2\right) + \frac{1}{2}\|x'_{n,1}\|^2 \\ &= \left(\frac{\widetilde{\omega}}{\omega}\right)^2 \left(I(x_n, \dot{x}_n) + \frac{\gamma}{2}\|\dot{x}_{n,1}\|^2\right). \end{aligned} \tag{45}$$

Similarly, we get for the Hamiltonian

$$\begin{aligned} \widetilde{H}(x_n, x'_n) &= \frac{1}{2}\Big(\|\dot{x}_{n,0}\|^2 + \|x'_{n,1}\|^2 + \widetilde{\omega}^2\|x_{n,1}\|^2\Big) + U(x_n) \\ &= H(x_n, \dot{x}_n) - I(x_n, \dot{x}_n) + \widetilde{I}(x_n, x'_n) \\ &= H(x_n, \dot{x}_n) + \frac{\gamma}{2}\|\dot{x}_{n,1}\|^2 + \left(1 - \frac{\omega^2}{\widetilde{\omega}^2}\right)\widetilde{I}(x_n, x'_n)\,, \end{aligned} \tag{46}$$

and hence (44) yields the result. □

For fixed $h\omega \geq c_0 > 0$ and $h \to 0$, the maximum deviation in the energy does not tend to 0, due to the highly oscillatory term $\frac{\gamma}{2}\|\dot{x}_{n,1}\|^2$. This term is bounded because of $\|\dot{x}_{n,1}\|^2 \leq \|x'_{n,1}\|^2 \leq 2\widetilde{I}(x_n, x'_n) \leq Const.$ It is possible to prove that the average over a fixed (sufficiently large) number of consecutive values $\|\dot{x}_{n,1}\|^2$ is constant.

Numerical experiments. We consider the FPU-type problem (with $\omega = 50$) discussed in the beginning of this lecture. Figure 8 shows the error in the total energy of the Störmer–Verlet method with four different step sizes. For the largest

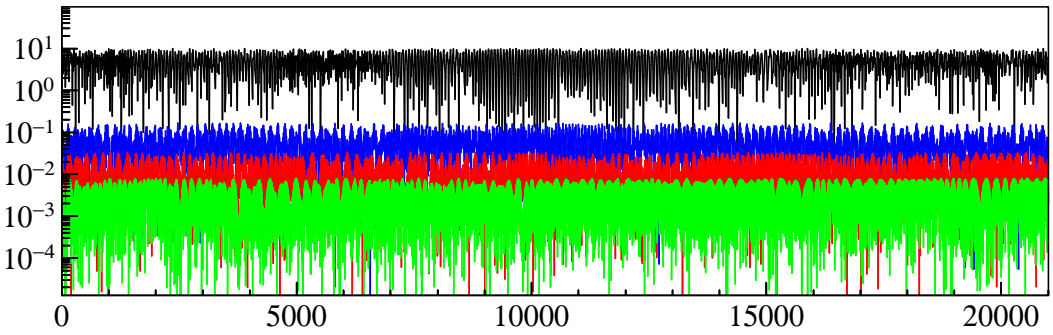

Figure 8: Error in the total energy of the FPU-type problem ($\omega = 50$) obtained for the Störmer–Verlet method applied with four different step sizes: $h\omega = 1.95, 1, 0.5, 0.25$.

step size (where $h\omega = 1.95$) the error is very large and of the size of $\gamma \approx 20$. Nevertheless, there is no drift in the energy. Halving the step size decreases the error by a factor close to 60. This is in good agreement with the form of the function $\gamma = \gamma(h\omega)$.

Our second experiment (Figure 9) shows again the energy error for various choices of ω and h. It illustrates the fact that the term $\frac{\gamma}{2}\|\dot{x}_{n,1}\|^2$ dominates the error (for large step sizes) and depends essentially on the product $h\omega$. We can also see that the error oscillates around a constant which is different from the theoretical value of the Hamiltonian.

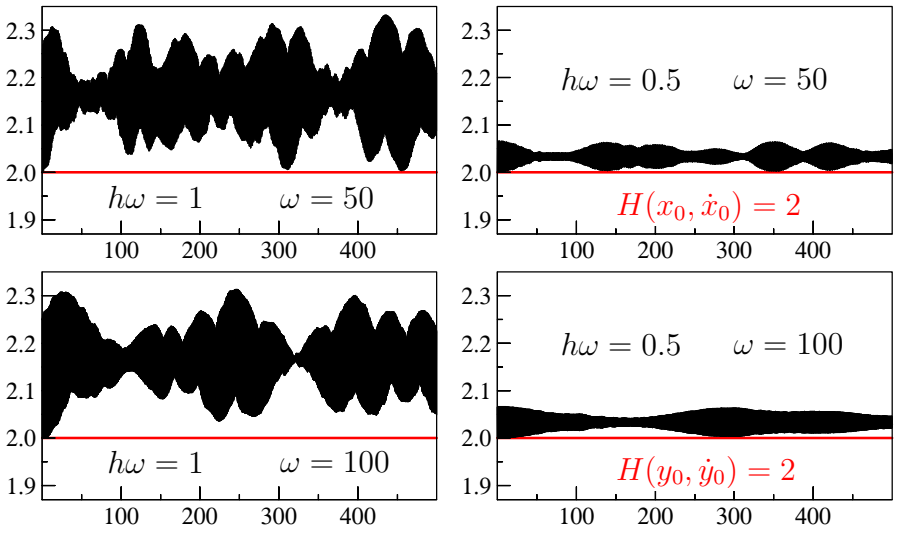

Figure 9: Total energy of the FPU-type problem along numerical solutions of the Störmer–Verlet method.

8 Exercises

1. Interpret the exponential integrator (9)–(10) as a splitting method: a half-step of a symplectic Euler type method for $\ddot{x} = g(x)$, a step of the exact solution for $\ddot{x} + \Omega^2 x = 0$, and finally the adjoint of the first half-step.

2. Show that a method (9)–(10) satisfying (11) is symplectic if and only if

$$\psi(\xi) = \mathrm{sinc}(\xi)\,\phi(\xi) \qquad \text{for} \quad \xi = h\omega.$$

3. The change of coordinates $z_n = \chi(h\Omega)x_n$ transforms (9)–(10) into a method of identical form with $\phi, \psi, \psi_0, \psi_1$ replaced by $\chi\phi, \chi^{-1}\psi, \chi^{-1}\psi_0$, $\chi^{-1}\psi_1$. Prove that, for $h\omega$ satisfying $\mathrm{sinc}(h\omega)\phi(h\omega)/\psi(h\omega) > 0$, it is possible to find $\chi(h\omega)$ such that the transformed method is symplectic.

4. Prove that for infinitely differentiable functions $g(t)$ the solution of the differential equation $\ddot{x} + \omega^2 x = x + g(t)$ can be written as

$$x(t) \;=\; y(t) + \cos(\omega t)\, u(t) + \sin(\omega t)\, v(t),$$

where $y(t)$, $u(t)$, $v(t)$ are given by asymptotic expansions in powers of ω^{-1}. *Hint.* Use the variation-of-constants formula and apply repeated partial integration.

5. Consider a Hamiltonian $H(p_R, p_I, q_R, q_I)$ and let

$$\mathcal{H}(p, q) \;=\; 2\, H(p_R, p_I, q_R, q_I)$$

for $p = p_R + \mathrm{i}p_I$, $q = q_R + \mathrm{i}q_I$. Prove that in the new variables p, q the Hamiltonian system becomes

$$\dot{p} = -\frac{\partial \mathcal{H}}{\partial \overline{q}}(p, q), \qquad \dot{q} = \frac{\partial \mathcal{H}}{\partial \overline{p}}(p, q).$$